Journal of Applied Physics

Conduction band caused by oxygen vacancies in aluminum oxide for resistance random access memory

Cite as: J. Appl. Phys. **112**, 033711 (2012); https://doi.org/10.1063/1.4745048
Submitted: 05 March 2012 . Accepted: 17 July 2012 . Published Online: 07 August 2012

Seisuke Nigo, Masato Kubota, Yoshitomo Harada, Taisei Hirayama, Seiichi Kato, Hideaki Kitazawa, and Giyuu Kido

Conduction band caused by oxygen vacancies in aluminum oxide for resistance random access memory

Seisuke Nigo,[1,a)] Masato Kubota,[2] Yoshitomo Harada,[1] Taisei Hirayama,[3] Seiichi Kato,[1] Hideaki Kitazawa,[1] and Giyuu Kido[1]
[1]*National Institute for Materials Science, 1-2-1 Sengen, Tsukuba, Ibaraki 305-0047, Japan*
[2]*Japan Atomic Energy Agency, 2-4 Shirane Shirakata, Tokai-mura, Ibaraki 319-1195, Japan*
[3]*Rigaku Corporation, 3-9-12 Matsubara-cho, Akishima, Tokyo 196-8666, Japan*

(Received 5 March 2012; accepted 17 July 2012; published online 7 August 2012)

As a next-generation memory, we have developed a rare-metal-free memory using Al oxide with a high-density of oxygen vacancies (V_os). The electronic structure has been simulated using first-principles calculations. In this paper, we report the electronic structure of the band gap, analyzed using thermally stimulated current measurements, to evaluate the simulated results. We observed electronic states corresponding to resistance changes for the first time. These results show that V_o^{+2} (electron empty V_o) changes to V_o^{+1} by electron injection; the overlapped V_o^{+1} electron changes into a "V_o conduction band" (V_oCB), and the changed structure is stabilized by structural relaxation of Al ions around V_o. V_oCB is considered as a kind of mid-gap impurity band. The origin of the on/off switching is considered to be generation/degeneration of the V_oCB caused by increasing/decreasing numbers of V_o electrons. Based on knowledge of the electronic mechanism, we have changed metal/insulator/metal structure to a metal/insulator/semiconductor structure and decreased the reset-current to 7 μA. The V_os of Al oxide are considered to be useful for electronic memory storage. © *2012 American Institute of Physics*. [http://dx.doi.org/10.1063/1.4745048]

I. INTRODUCTION

Resistance random access memory (ReRAM), as the next-generation memory to succeed flash memory, is being developed using many kinds of transition-metal oxides.[1] However, the switching mechanisms are not yet fully clear. The switching mechanism of a transition-metal-oxide ReRAM is believed to be caused by O ion migration.[2] Recently, it was clarified by x-ray photoelectron spectroscopy (XPS) that a small XPS energy shift occurs by redox reactions, such as $2TaO_2 + O^{2-} \leftrightarrow Ta_2O_5 + 2e$.[3,4] However, the electronic state itself has not yet been observed. We have developed ReRAM using Al anodized oxide (AlOx) instead of a transition-metal oxide, focusing on oxygen vacancies (V_os) localized in the AlOx cell boundaries.[5]

Pioneering researches on the electronic properties of anodized AlOx have been continued systematically since 1964 by Hickmott. He proposed energy-band diagrams of impurity bands with double Schottky barriers of structure Al/AlOx/Au and reported the existence of defects at a density of $10^{19}-10^{20}$ cm^{-3} with a broad energy distribution among the band gaps of AlOx.[6] His detailed researches showed that defects are introduced at the time of anodization, and that electrons were injected from the Al electrode into AlOx by Fowler–Nordheim (FN) tunneling.[7] The negative resistance phenomenon of AlOx discovered by Hickmott[8] is considered to lead directly to resistive switching of AlOx-ReRAM. However, since he used an anodized AlOx film as thin as 28 nm, a cell boundary did not exist, and therefore no attention was paid to V_os localized at the cell boundary. As a result, the switching mechanism caused by a high-density of V_os, such as 10^{21} cm^{-3}, was overlooked until our research. Theoretically supporting our research, Momida *et al.* simulated the electronic structure of amorphous alumina containing a high-density of V_os using first-principles calculations for the first time and the simulation results have been published.[9]

In this paper, we report an experimental study of the electronic states, analyzed using the thermally stimulated current (TSC), to evaluate the V_o conduction band (V_oCB) model, based on the simulation results. Next, we show a metal/insulator/semiconductor (MIS) AlOx-ReRAM structure developed with the aim of significantly reducing the reset-current. In addition, to understand the resistive switching mechanism driven by injection/extraction of electrons, we show schematically the electronic state changes among the band gaps using TSC spectra and a band model. Finally, we propose using a dry-type AlOx film, similar to the cell boundary, instead of anodized AlOx, which is not suitable for semiconductor manufacturing processes. Generally, a switching mechanism driven by electron injection/extraction is advantageous compared with the ion-migration mechanism of other types of ReRAM with respect to cycle endurance and power saving.

II. EXPERIMENT

An Al(top)/AlOx/Al(bottom) memory cell was fabricated. First, a 0.5-mm-thick Al sheet (99.99%) was treated by electrochemical polishing in a mixed solution of perchloric acid and ethanol. The Al sheet was anodized using a two-step anodization process.[10] The Al sheet was anodized at a voltage of 40 V in oxalic acid (0.3 M) at 293 K for 3 h.

a)Author to whom correspondence should be addressed. Electronic mail: NIGO.Seisuke@nims.go.jp.

Then, the anodic oxide layer was removed in a mixture of phosphoric acid (6 wt. %) and chromic acid (1.8 wt. %) at 333 K for 1 h. The Al sheet was then anodized again for 64 s under the same conditions as in the first step. After drying, an Al electrode of thickness 80 nm with a diameter of 300 μm was formed using a heat evaporation system, and Cu wire was bonded with Ag paste. An Al (top)/AlOx/p^+-Si (bottom) memory cell was fabricated as a MIS-type ReRAM. The native oxide on the surface of the p^+-Si wafer (boron high-doped Si, 0.001–0.005 Ω cm) was removed using a solution of 1% HF (10 min), and Ar-ion sputtering (DC 100 W, 1 min). An Al thin film of thickness 200 nm sputtered on the p^+-Si wafer was anodized using the same conditions as in the second step of production of the Al/AlOx/Al memory cell. The subsequent processes were the same as the processes in production of the Al/AlOx/Al memory cell. An anodized Al sheet was vertically sliced to a thickness of 100 nm using a focused ion-beam (Hitachi FB-2000 A). The sliced samples were observed using transmission electron microscopy (TEM) at 200 kV (JEOL JEM-2100 F). A planar section of the AlOx film was observed using high-resolution TEM (Hitachi H9500). The electronic structures of specimens of thickness 70 nm were determined using electron-energy-loss spectroscopy (EELS; Gatan GIF/Model 863), with a beam spot diameter of 1 nm. The localized existence of AlOx oxygen vacancies was determined, as shown in Fig. 1. The *I–V* characteristics were measured using a source-meter unit (Keithley 2400). A current-regulating diode (CRD) of 28 μA was inserted in series to the measuring circuit. The sweep range, the sweep speed, and the step size were ±3 V, 0.5 V s^{-1}, and 0.5 V, respectively. The electronic state of the off-state sample of the Al/AlOx/Al memory cell was measured using a TSC measurement system (Rigaku TSC-FETT 2000). The sweep range, the rate of temperature increase, and the applied voltage were 80–550 K, 0.15 K s^{-1}, and 0 V, respectively.

III. RESULTS AND DISCUSSIONS

A. Oxygen vacancies and electronic state analysis

First of all, in the case of AlOx-ReRAMs, unlike transition-metal oxide ReRAMs, such as Pt/Ta_2O_{5-x}/TaO_{2-x}/Pt, we considered that the origin of the resistive switching is an increase/decrease in V_o electrons rather than O ion movement. Nanoholes and cell boundaries are generated by self-formation in the Al anodization process. The existence of localized V_os in the cell boundary of AlOx was revealed by the O K-edge spectra satellite peak in EELS as follows. The cell boundary is visible as light gray lines of width approximately 20 nm in the TEM image shown in Figs. 1(b) and 1(c). A satellite peak at 534 eV is observed at the cell boundary at point B in Fig. 1(d), although it is not observed at points A and C. Furthermore, as shown in Fig. 1(e), the EELS depth profile indicates that satellite peaks exist continuously in region E but not in regions D and F of the vertical cell boundary. Generally, the satellite peak at 534 eV is considered to be caused by V_os of the metal oxide. We focused on the V_os as useful electronic storage sites.

The above-mentioned simulation results (Ref. 9) suggest that V_o^{+2} (electron empty V_o) changes to V_o^{+1} (electron half-filled V_o) as a result of electron injection in the case of V_o^{+1} densities of 10^{21} cm^{-3} or more; overlapped V_o^{+1} electrons generate a V_oCB among the band gaps of AlOx. The changed electronic state is stabilized by local atomic relaxations around the V_os, as shown in Fig. 2(a). A model of the "V_o pseudo-cluster" is $Al_3O_{12}(V_o)_1$, in which three Al atoms are located around one V_o and each Al atom is surrounded by four O atoms, and is part of a super-cell of 120 atoms; the model was simulated using an $Al_{48}O_{72}$ crystal structure as a typical semi-stable amorphous structure, using molecular dynamics (see Ref. 9 for details). An electron trapped at a V_o site is localized in this state and oozes out to 12 O atoms around the V_o^{+1}, as shown in yellow in Fig. 2(a). Therefore,

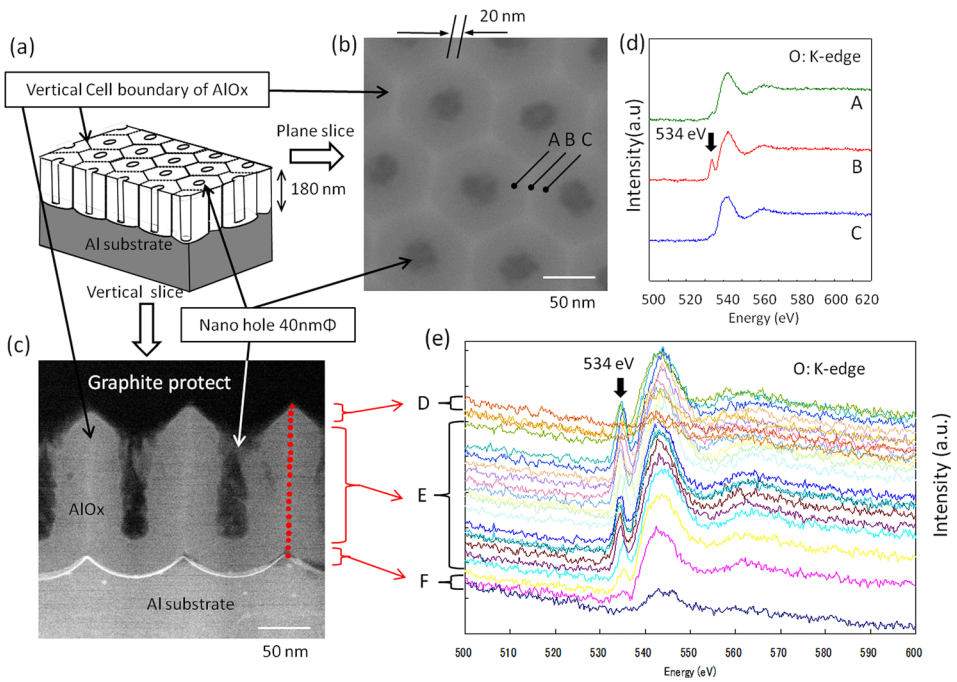

FIG. 1. Oxygen vacancies localized at the cell boundary of AlOx. (a) Schematic cross-section of AlOx. (b) AlOx plane TEM image. (c) AlOx vertical TEM image. (d) and (e) EELS spectra of O K-edge measured at A, B, C and every red point. D: Surface of AlOx, E: inner domain, F: interface of Al substrate. Arrow indicates satellite peaks caused by oxygen vacancies of AlOx.

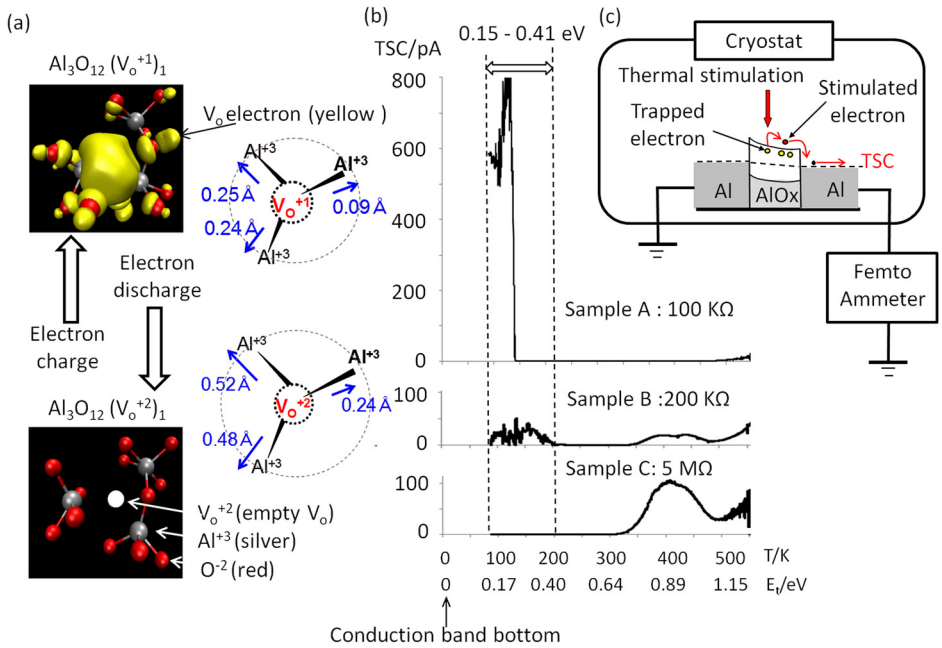

FIG. 2. Structural change in V_o cluster and TSC measurements. (a) Structural relaxation of Al ions around the V_o by one electron charge/discharge. Blue numerical values show Al-V_o distance changes (V_o^0 base) by first-principle calculation. (b) TSC of off-state of 100 KΩ, 200 KΩ, and 5 MΩ. (c) Illustration of TSC method.

the bound energy of the inner-shell electron of the O atom is considered to be decreased by the charge of the V_o^{+1} electron. As a result, the O K-edge of the EELS spectrum shifts towards a lower energy. This energy shift is considered to be part of the probable origin of the satellite peak of EELS shown in Fig. 1. Although further research is required for confirmation, the V_o^{+1} electron shown in yellow in Fig. 2(a) seems to be an electron with a broad distribution in a cluster consisting of three Al atoms, 12 O atoms, and one V_o. V_o^{+1} electrons are considered to be delocalized by increasing in number and overlapping spatially, generating V_oCB.

TSC measurements are used to detect impurity levels in semiconductors or insulators. Trapped electrons at impurity levels at a low temperature, such as 80 K, are excited up to the conduction band by constant heating and emitted to the electrode. The current emitted to the measurement circuit is recorded against temperature, providing information on the energy of trapped electrons and holes. A diagram of a TSC measurement system is shown in Fig. 2(c). Generally, delocalized electrons cannot be measured by TSC, although localized electrons and holes can be measured precisely by TSC. As a trial, we measured an on-state sample of an AlOx-ReRAM of approximately 10 Ω; the measurement was impossible because of the noise current of 0.1 mA induced by the femto-ammeter. The horizontal axis of Fig. 2(b) is the activation energy of the trapped electron (E_t), calculated using the following equation:[11]

$$E_t = kT_m \ln(T_m^4/\beta), \quad (1)$$

where k is the Boltzmann constant, T_m is the TSC peak temperature, and β is a heating rate of 0.15 K s^{-1}. We show, here, three typical electronic states, measured using the TSC method, as electronic states of different resistances in the off-state sample of AlOx-ReRAM, as shown in Fig. 2(b). In detail, it became clear that electronic states 0.15–0.41 eV below the framework conduction band (FCB) are generated, corresponding to decreases in resistance. Electronic states in this energy range do not exist in sample C but exist in the cases of samples A and B. If the number of V_o^{+1} electrons increases more than that of sample A, V_oCB will be generated by delocalization of V_o^{+1} electrons, and simultaneously, the electronic state will change to metallic conduction; i.e., the electronic state 0.15–0.41 eV below the FCB is considered as a bud of the V_oCB or remains of the V_oCB. It is therefore presumed that these electronic states change into the V_oCB by increasing the number of V_o^{+1} electrons. We show these electronic state changes later, in Fig. 5.

The origin of the switching mechanism of a transition-metal oxide ReRAM was revealed by XPS, as mentioned above. Although we tried using XPS measurements to detect the binding-energy shift of AlOx, we failed. This is because the change occurs not in bulk but in the nanodomain of the cell boundary of width ~20 nm, as shown in Fig. 1(b), so the XPS signal is so small that it is undetectable. On the other hand, we directly observed a clear change in the electronic state using the TSC method for the first time, as mentioned above. Since the V_o^{+1} electron exists at a level 0.15–0.41 eV below the FCB, the electron is expected to provide long-term electronic storage. However, it becomes difficult to extract the V_o^{+1} electron by electronic excitation up to the FCB. In other words, a feature of AlOx-ReRAM is an easy set-operation and a difficult reset-operation, which is similar to other types of ReRAM.

B. Resistive properties and *I–V* characteristics of metal/insulator/metal (MIM) type AlOx-ReRAM

A typical unipolar-type *I–V* curve of a memory cell is shown in Fig. 3(c); it was measured by changing the voltage at room temperature as follows: 0 → +3 → 0 → +2 → 0 V. The high-resistance state (HRS) becomes a low-resistance state (LRS) at 2.5 V in the process of which it increases to 3 V, and the current is limited to 28 μA by a CRD, as shown

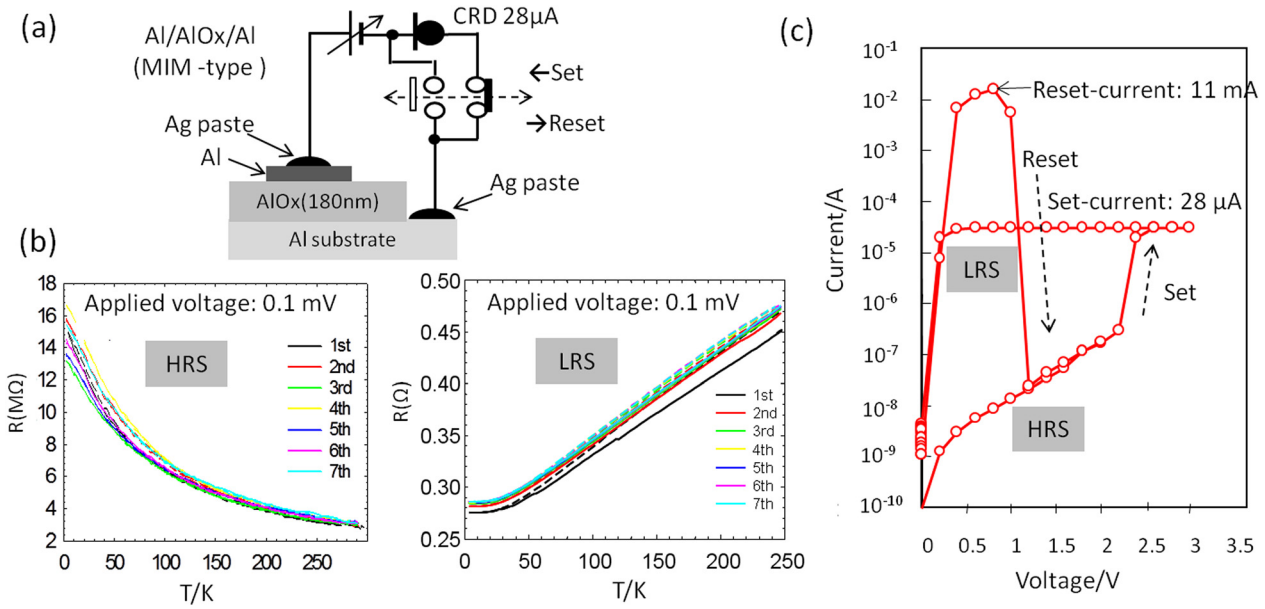

FIG. 3. Resistive properties of AlOx-ReRAM memory cell. (a) Basic structure of MIM-type of AlOx-ReRAM, and measurement circuit with a CRD. (b) Resistance change with temperature in HRS and LRS. (c) Typical unipolar-type *I-V* characteristics. Set current limited to 28 μA by CRD.

in Fig. 3(c). Subsequently, by increasing the applied voltage to 2 V without the CRD, a larger reset-current than the set-current changes LRS to HRS at 1.2 V.

Based on the temperature dependence of resistance shown in Fig. 3(b), it was clear that the conduction mechanism in the HRS is a state of hopping conduction, in which the resistance increases exponentially with decreasing temperature, and the conduction mechanism in the LRS is a metallic conduction in which the resistance decreases linearly with decreasing temperature. Since the LRS is reset to HRS if the current increases to the reset-current as a result of a decrease in temperature, the increase in current accompanying a decrease in temperature must be controlled to be smaller than the reset-current. We therefore measured the temperature dependence of the resistance (Fig. 3(b)) with a voltage of only 0.1 mV. In the case of unipolar drive, a larger current than the set-current causes a reset mechanism, as shown in Fig. 3(c). The restriction that the reset-current must be larger than the set-current is a fatal fault of low-power-consumption memory.

C. MIS-type AlOx-ReRAM and mechanism study

To reduce the reset-current significantly, we developed a MIS-type AlOx-ReRAM with a bipolar drive, as shown in Fig. 4(a). Since the origin of the on/off switching is considered to be generation/degeneration of V_oCB by increasing/decreasing the numbers of V_o electrons, blocking the inflow of current at the time of reset is considered to be effective in reducing the reset-current. We therefore changed the structure from a MIM-type Al/AlOx/Al to a MIS-type Al/AlOx/p^+-Si and were able to decrease the reset-current to 7 μA using a p–n junction, as shown in Fig. 4(b).

In addition, we show in Fig. 4(c) a schematic illustration of the on/off sequential mechanism based on the V_o band models to help understand the MIS-type AlOx-ReRAM.

By increasing the applied voltage to the threshold value V_{on}, the electron that passed the Schottky barrier by FN tunneling is trapped at V_o^{+2}. V_o^{+2} changes into V_o^{+1}, and the energy level of V_o^{+1} falls to the band gap from the FCB bottom simultaneously with electron trapping, as shown in Fig. 4(c-1). The changed electronic structure is stabilized by shrinking of the Al ions around the V_o. As a result of increasing the number of V_o^{+1} electrons, the V_o^{+1} electrons overlap and delocalize, and the conductive electronic state of V_oCB is generated, as shown in Fig. 4(c-2). This state is the on-state of metallic conduction, caused by V_oCB. The set-mechanism is considered to be as shown in Eq. (2). By increasing the reverse voltage, since the reverse current is prevented by the p–n junction, V_o electrons are instantly extracted by a reverse electric field. The reset-mechanism is considered to be as shown in Eq. (3); the state is stabilized by the spreading of Al ions, and the energy level of V_o^{+2} increases to near the FCB bottom, as shown in Fig. 4(c-3). The V_o^{+1} electrons are localized as a result of their decreasing number. Simultaneously, the metallic conduction returns to band-insulator hopping conduction, as shown in Fig. 4(c-4). The spreading and shrinking of Al ions around the V_o correspond to changes in the Al-V_o distance shown in Fig. 2(a). The aforementioned mechanisms can be expressed simply as follows:

$$V_o^{+2} + e^- \rightarrow V_o^{+1} : \text{reduction of } V_o \text{ by electron injection} \rightarrow \text{on-state by delocalized } V_o \text{ electrons} \quad (2)$$

$$V_o^{+2} \leftarrow V_o^{+1} - e^- : \text{oxidation of } V_o \text{ by electron extraction} \rightarrow \text{off-state by localized } V_o \text{ electrons} \quad (3)$$

These reactions are accompanied by a sub-reaction in which the electronic structure of V_o is stabilized by structural relaxation of Al ions around the V_o. The aforementioned simulation results show that structural relaxation of amorphous AlOx is larger and more stable than that of crystalline Al_2O_3,

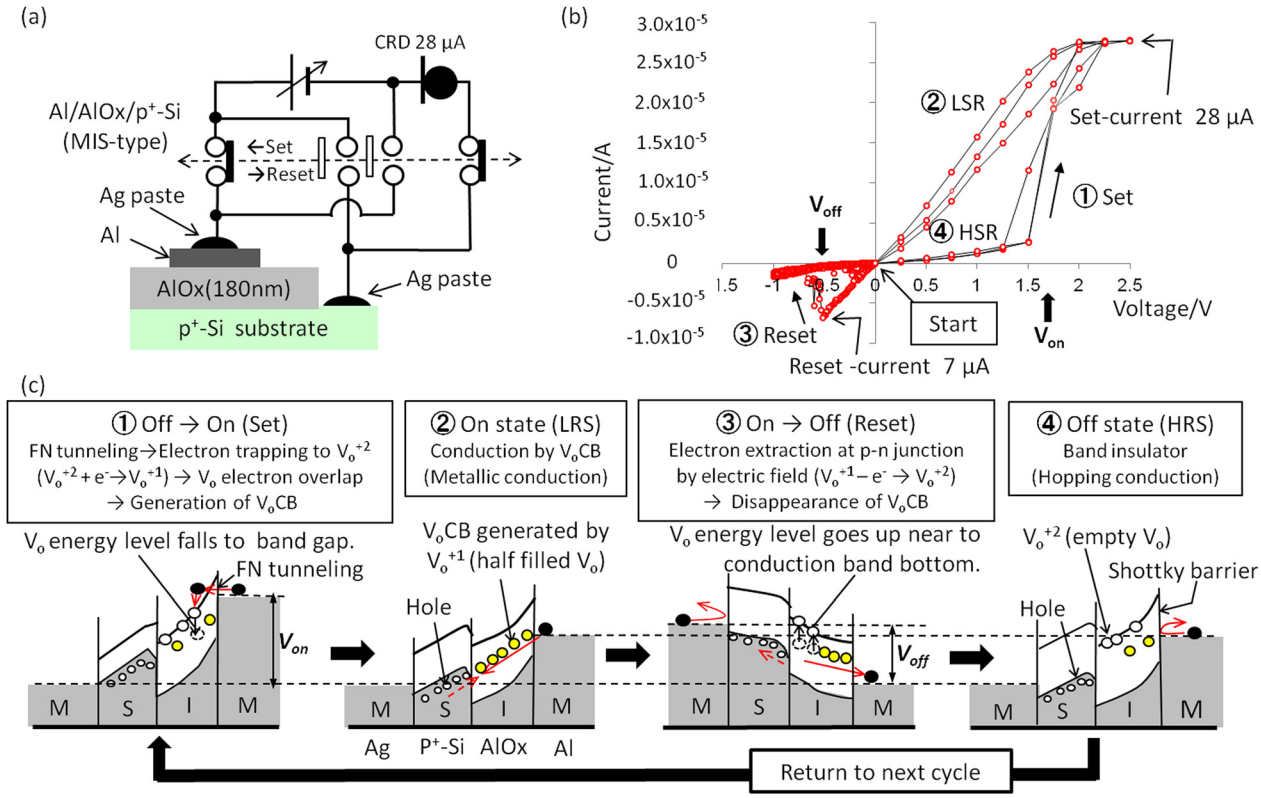

FIG. 4. MIS-type AlOx-ReRAM and a mechanism image. (a) *I-V* characteristic measurement circuit with CRD. (b) Typical bipolar-type *I-V* characteristic of three cycles. Set current is limited to 28 μA by CRD. Reset current is decreased to 7 μA by p-n junction effect. (c) An image of on/off mechanism based on the band model. Sequence numbers 1-4 in Fig. 4(c) are corresponded to the numbers 1-4 in Fig. 4(b).

i.e., a bistable electronic structural change in crystalline Al_2O_3 does not occur, even if it contains a high-density of V_os (see Ref. 9 for details).

Two reactions, $V_o^{+2} + e^- \rightarrow V_o^{+1}$ and $V_o^{+2} + 2e^- \rightarrow V_o^0$, progress simultaneously as a result of electron injection. V_o^0 is non-conductive, because of full electronic occupation, and does not participate in resistance changes. The generation of a V_oCB as a result of an increase in the number of V_o^{+1}s decreases the effective voltage, and electron injection by FN tunneling stops because the Schottky barrier is revived by a decrease in the effective voltage, i.e., the reaction $V_o^{+2} + 2e^- \rightarrow V_o^0$ does not contribute to the resistance change.

In 2002, Hickmott reported 10 metal oxides, namely, Ta_2O_5, PrO_x, TiO_2, Nb_2O_5, ZrO_2, SiO, CeO_2, MgO, Y_2O_3, and anodized Al_2O_3, that show negative resistance.[12] In recent years, all the metal oxides listed by Hickmott have been verified by many researchers to be candidate materials for ReRAM. In general, defects have adverse effects on semiconductors, and therefore the removal of defects, such as V_o is important. However, in the case of AlOx-ReRAM, high-density V_o in anodized Al_2O_3 is considered to serve as useful electronic storage sites for electron injection/extraction.

D. Electronic structure change study

To help further understanding of the electronic structures of AlOx-ReRAM, Fig. 5 shows a schematic diagram of the electronic structures of the on/off state, based on TSC analyses. The electronic states of typical off-states, based on Fig. 2(b), are shown in the orange area in Fig. 5. TSC measurement of the on-state is impossible because of delocalized electrons. The electronic state of the on-state was therefore presumed, based on clear tendencies of changes in the off-state, to be as follows. In the case of a high resistance of 5 MΩ, electrons do not exist in the energy range 0.15–0.41 eV below the FCB, as shown in Fig. 5(a-1). However, when the resistance decreases from 5 MΩ to 200 KΩ, electrons appear in the energy range 0.15–0.41 eV below the FCB, as shown in Fig. 5(a-2). Furthermore, when the resistance decreases from 200 kΩ to 100 kΩ, the TSC increases sharply in a narrower part of the same energy range, as shown in Fig. 5(a-3). If the resistance decreases to 100 Ω or less, TSC measurements become impossible because of delocalized electrons. Such a state is a delocalized electronic state, namely, the on-state. Since TSC is measured in the temperature range above 80 K, the electronic state in the range 0–0.15 eV below the FCB cannot be revealed using TSC. The number of electrons near the measurement limit of 0.15 eV below the FCB increases sharply, corresponding to a decrease in the resistance, as shown in Fig. 2(b). The delocalized electrons caused by an increase in the number of electrons are therefore also considered to exist above the level of 0.15 eV below the FCB. Since V_oCB is generated with the delocalized electrons, the Fermi level (E_f) of the on-state is considered to exist at a level above 0.15 eV below the FCB, as shown in Fig. 5(b).

Although the electronic states in the band gap, except at 0.15–1.28 eV below FCB, are not clarified, a band gap of 6.5 eV was clarified by EELS measurements of the AlOx cell

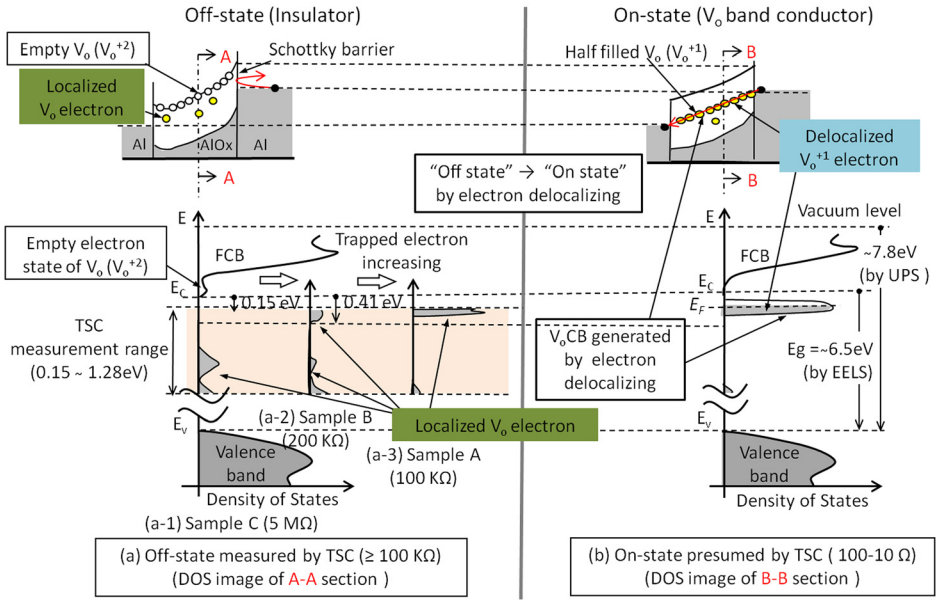

FIG. 5. Schematic illustrations of electronic structures of on/off-state based on TSC. (a) Electronic states 0.15-1.28 eV below the conduction band measured by TSC are shown in the orange area as typical off-states. DOS patterns are TSC curves rotated to the right through 90°. (b) Electronic state of on-state is estimated from tendencies in changes in the off-state. FCB and VoCB denote the framework conduction band and the V_o conduction band, respectively. A-A and B-B arrows indicate the cross-section line of the schematic energy-band diagram of Al/AlOx/Al structure corresponding to the on/off-state.

boundary. The valence band top level of AlOx, estimated using UV photoelectron spectroscopy (UPS), exists at 7.8 eV below the vacuum level, and the shape of the valence band near the top of AlOx is similar to the valence band of crystalline Al_2O_3. To summarize these measurement results for electronic states, a schematic diagram of the on/off-state electronic structures of AlOx-ReRAM is shown in Fig. 5.

Finally, since a dry process is more suitable in semiconductor manufacturing process than a wet-type anodization process, we are extending our research to a sputtered AlOx film, based on knowledge of the cell boundary of anodized AlOx. Although the production process of AlOx does not need to be anodization, the electronic structure must be similar to the cell boundary of anodized AlOx, containing a high-density of V_os, i.e., 10^{21} cm^{-3} or more. A remarkable feature of V_os is the ability to receive and release electrons with structural relaxation, without any chemical reaction.

IV. CONCLUSIONS

We showed a resistive switching mechanism of an AlOx-ReRAM based on the electronic states revealed by TSC. This system is expected to have high endurance, equivalent to that of dynamic random access memory (DRAM), because it is driven by increasing/decreasing numbers of electrons, similar to DRAM. To verify the mechanism, and decrease the reset-current, we changed a MIM-type AlOx-ReRAM to a MIS type, and decreased the reset-current to 7 μA, as expected. Although the properties of materials with high-density V_os are still under study, in the future, V_o host materials may be not limited to AlOx; well-designed V_o materials are expected to provide excellent and rare-metal-free electronic materials.

ACKNOWLEDGMENTS

This work was performed under a subsidy from the Elements Science and Technology Project of MEXT, Japan. The authors are grateful to Kobelco Research Inc. and the Fukuryo Semicon Engineering Co. for TEM and EELS measurements.

[1]A. Sawa, Mater. Today **11**, 28 (2008).
[2]M.-J. Lee, C. B. Lee, D. Lee, S. R. Lee, M. Chang, J. H. Hur, Y.-B. Kim, C.-J. Kim, D. H. Seo, S. Seo, U.-I. Chung, and I.-K. Yoo, Nature Mater. **10**, 625 (2011).
[3]C. Yoshida, K. Kinoshita, T. Yamasaki, and Y. Sugiyama, Appl. Phys. Lett. **93**, 042106 (2008).
[4]Z. Wei, Y. Kanzawa, K. Arita, Y. Katoh, K. Kawai, S. Muraoka, S. Mitani, S. Fujii, K. Katayama, M. Iijima, T. Mikawa, T. Ninomiya, R. Miyanaga, Y. Kawashima, K. Tsuji, A. Himeno, T. Okada, R. Azuma, K. Shimakawa, H. Sugaya, T. Takagi; R. Yasuhara, K. Horiba, H. Kumigashira, and M. Oshima, Int. Electron Devices Meet. **2011**, 04796676.
[5]J. Lee, S. Nigo, Y. Nakano, S. Kato, H. Kitazawa, and G. Kido, Sci. Technol. Adv. Mater. **11**, 025002 (2010).
[6]T. W. Hickmott, J. Appl. Phys. **100**, 083712 (2006).
[7]T. W. Hickmott, J. Appl. Phys. **97**, 104505 (2005).
[8]T. W. Hickmott, J. Appl. Phys. **106**, 103719 (2009).
[9]H. Momida, S. Nigo, G. Kido, and T. Ohno, Appl. Phys. Lett. **98**, 042102 (2011).
[10]H. Masuda and K. Fukuda, Science **268**, 1466 (1995).
[11]Z. Fang, L. Shan, T. E. Schlesinger, and A. G. Milnes, Mater. Sci. Eng. B **5**, 397 (1990).
[12]T. W. Hickmott, J. Appl. Phys. **88**, 2805 (2000).